Vol. 44, No. 2, pp 191-197, 2016
Indian Journal of Soil Conservation
Online URL:http://indianjournals.com/ijor.aspx?target=ijor:ijsc&type=home

Application of SEBAL model to estimate Evapotranspiration in Doon Valley, India

C. Jana[1], Monika Rawat, D.R. Sena, N.M. Alam, U. Mandal, R. Kaushal and P.K. Mishra

ICAR-Indian Institute of Soil and Water Conservation, Dehradun-248195, Uttarakhand.

[1]*E-mail:chayna_4503@yahoo.co.in*

ARTICLE INFO

Article history :
Received : October, 2014
Revised : November, 2014
Accepted : July, 2016

Key words :
Doon Valley,
Evapotranspiration,
GIS,
Remote sensing,
SEBAL

ABSTRACT

The knowledge of actual water use for different land uses particularly for agricultural crops is considered as one of the major factors for water resource planning and irrigation water management. However, actual water use of a land use is mainly determined by its actual evapotranspiration (ET_a). In recent times, with the advent of new satellite technology, spatio-temporal evapotranspiration can be measured from remotely sensed surface temperature using various surface energy balance algorithms.In this study, SEBAL (Surface Energy Balance Algorithm for Land) techniquehas been used to measure the spatial variation of actual evapotranspiration (ET_a) from Landsat 5 image prevailing in the Doon Valley, Uttarakhand, India. This particular method utilizes the combination of meteorological observations with information extracted from remote sensing data to calculate evapotranspiration and other energy exchanges at earth's surface. The result shows that SEBAL ET_a varies between 3.3 mm day^{-1} and 4.9 mm day^{-1} in the study area. The estimated ET_a was compared with the vegetation indices and surface temperature to see their variations among the classified land cover classes. Terraced agriculture has the highest ET (4.9 mm day^{-1}) partly due to its crop growth stage as compared to other land cover classes. Spatio-temporal distribution of actual ET can assist us to better understand evapotranspiration pattern of different land use systems and would help to establish links between land use, water allocation, and water use planning.

1. INTRODUCTION

As fresh water becomes scarcer, demands for fresh water is increasing over the time, therefore judicious water resource planning will be very much needed in coming days to achieve greater efficiency in the use of this valuable resource. In agricultural system, the actual evapotranspiration of crops is one of the most useful indicators for optimizing crop production. The processes where water is lost to the atmosphere due to evaporation from the soil and transpiration from vegetation is referred to as evapotranspiration (ET). Evapotranspiration is also an important factor for hydrologic modeling and irrigation scheduling (Rogers *et al.,* 1983). The capability to predict levels of ET would be a valuable asset for water resource managers. Besides this, ET is a good indicator of irrigation effectiveness and total water consumption from vegetation. Unfortunately, under actual field conditions ET estimation is still a very challenging job for researchers and water managers (Petra *et al.,* 2010). It is affected by some processes at the interface between the soil, vegetation and the atmosphere.

The conventional way to compute ET is mainly based on climate data where collected climate data are used to estimate ET for a reference crop alfalfa. Then, crop water requirement for different crop stages is measured using area specific crop coefficient (K_c). There are many methods available to estimate reference ET using meteorological data: FAO-24 (Doorenbos and Pruitt, 1977), FAO-56 (Allen *et al.* , 1998). Reference ET can be defined as the ET rate of a reference crop expressed in inches or millimeters. All these models have increased the precision of ET estimation (Brutsert, 1979) over the times. But, most of these methods are based on point data, which do not provide a good estimation of ET for large areas (Tuya *et al.*, 2005)and often it is not practically feasible to capture all the spatial variation at broad scales.

The problem of ET estimation over a large area can be solved using remote sensing and GIS technology that provide ET on pixel-by-pixel basis. It is able to provide a large and continuous spatial coverage within a few minutes. It is also less expensive to retrieve the same spatial information than conventional measurements and the only approach for ungauged areas where man-made measurements are extremely difficult to conduct.

During the last two to three decades, significant progress has been made to estimate actual evapotranspiration (ET_a) using satellite remote sensing (Bastiaanssen *et al.*, 2002; Farah *et al*., 2004;Kustas*et al*., 2003; Kustas and Norman, 1996;Majnooni-Heris*et al*., 2012). These methods provide a powerful means to compute ET_a from the scale of an individual pixel right up to an entire raster image.

The SEBAL model has been used in several studies in many countries around the world and it was validated with high accuracy (Spiliotopoulos *et al.*, 2008; Bandara 2006; Bastiaanssen *et al.* , 2005; Alexandridis and Chemin 2001). It is more attractive for operational applications (Majnooni-Heris *et al.,* 2012; Papadavid *et al.*, 2013; Zohu *et al*., 2014). SEBAL uses digital image data collected by remote-sensing satellites that record thermal infrared, visible and near-infrared radiation for computing ET_a on a pixel-by-pixel basis for the instantaneous time of the satellite image. The process is based on a complete energy balance for each pixel, where AET is predicted from the residual amountof energy remaining from the classical energy balance.

SEBAL is one of the energy budgeting techniques popularly used to estimate actual evapotranspiration from satellite data (Bastiaanssen *et al.,* 1998). It combines empirical and physical parameterization using inputs from local weather data and satellite data (radiance). From the input data, the R_n (net solar radiation), Normalized Difference Vegetation Index (NDVI), albedo, roughness length, and G (soil heat flux) are calculated. The sensible heat flux is calculated by contrasting two points designated as '*cold*' (wet, well-irrigated vegetation) and '*hot*' pixels (dry barren ground). Then, the ET_a is calculated as the residual of the energy budget (Bastiaanssen *et al*., 1998, 2005).

SEBAL has been used globally for various applications related to irrigation planning and other agricultural water use (Liou and Kar, 2014). In the context of Indian sub-continent the application is obscure and limited. Given the fact that, the urbanisation, industrialisation and biotic interferences in the Doon Valley and its peripheral areas have adversely affected the agriculture in recent years due to competing share of water, application of SEBAL as a tool should be given impetus to monitor the water use gaps in agricultural sector. Further, the flagship PMKSY (*Pradhan Mantri Krishi Sichai Yojana*) program of the Govt. of India requires real time monitoring of the green water use as a basis of strengthening the irrigation infrastructure and scheduling water delivery on a priority basis, is going to be benefited with this technique immensely. Therefore, this manuscript attempts to explore the possibility of application of this technique on a pilot basis in the study area with validation from secondary information.

2. MATERIALS AND METHODS

Study Area

Doon Valley is located between $30^0$26'65" N to $30^0$02'58.06" N latitudes and $77^0$39'06.87"E to $78^0$19'23.61" E longitudes within the Shivalik Hills in the Lower Himalayas, in the state of Uttarakhand, India. The climate of the study area is sub-tropical with predominant spells of hot summer and cold winter (Jana *et al.,* 2015). Doon Valley has a rich vegetation cover. Although the major portion of this valley is occupied by forest land use with dominant forest species 'Sal' (*Shorearobusta*) (66.13%) followed by cultivated area (17.12%).

Data

Remote sensing data for 2010 November 13 (Landsat TM 5 with 30 m resolution) downloaded from https://earthexplorer.usgs.gov/ was used as a primary image for this study with an overpass time of 05:08:14 AM. Meteorological data were procured from weather station of ICAR-IISWC, Research Farm located at Selaqui, Dehradun for estimation of reference ET. The Doon Valley (Fig.1) consists of two watersheds; one outlet bounding to 'The Yamuna River' and other outlet to 'The Ganga River'. For this study, ASTER DEM (30m) data was used to derive topographic elevation data used in the technique.

SEBAL Model

The theoretical and computational basis of SEBAL is described in Bastiaanssen *et al*., 1998; Bastiaanssen, 2000; and Bastiaanssen *et al*., 2005. In the SEBAL model, ET is computed from satellite images and weather data using the surface energy balance as illustrated in Fig. 2. Since the satellite image provides information for the overpass time only, SEBAL computes an instantaneous ET flux for this overpass time. The ET flux is, then, calculated for each of the pixels of the image as a "residual" of the surface energy budget equation:

$$\lambda_{ET} = R_n - G - H \qquad ...(1)$$

Where, λ_{ET} is the latent heat flux (W/m^2), R_n is the net radiation flux at the surface (W/m^2), G is the soil heat flux (W/m^2), and H is the sensible heat flux to the air (W/m^2).

The net radiation flux at the surface (R_n) represents the actual radiant energy available at the surface. It is computed by subtracting all outgoing radiant fluxes from all incoming radiant fluxes. This is given in the surface radiation balance equation:

$$R_n = RS\downarrow - \alpha RS\downarrow + RL\downarrow - RL\uparrow - (1-\varepsilon_o)RL\downarrow \quad \ldots(2)$$

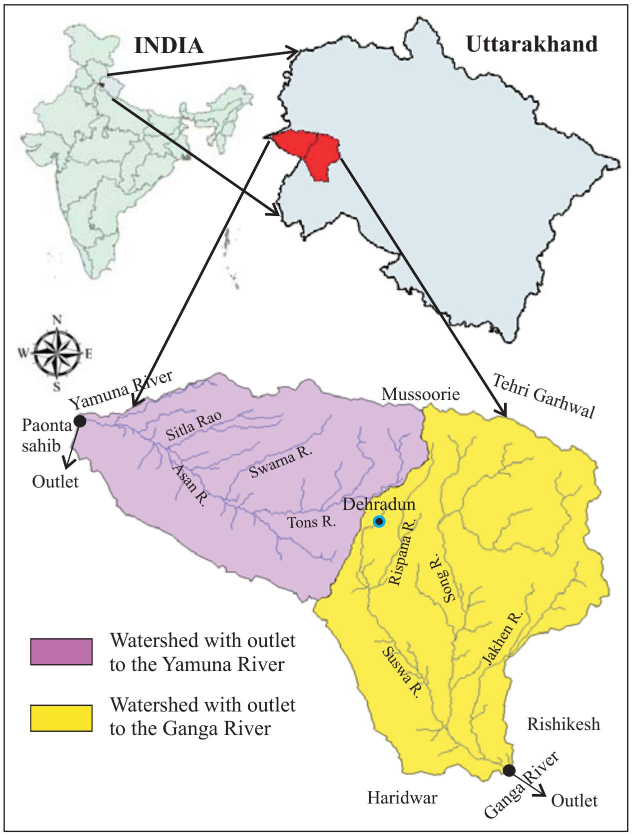

Fig. 1. Location of the study area

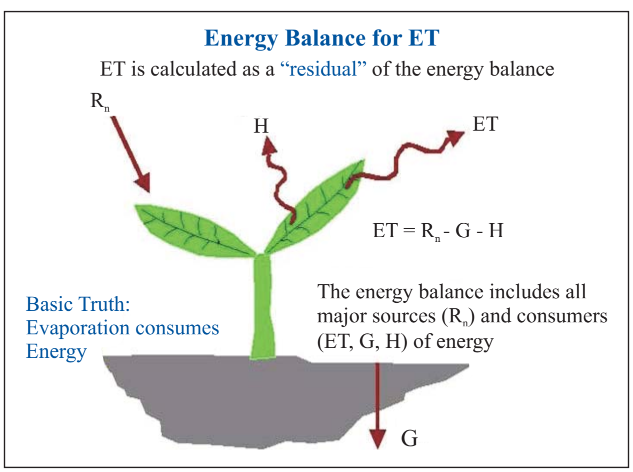

Fig. 2. Surface Energy Balance

Where, $RS\downarrow$ is the incoming shortwave radiation (W/m^2), α is the surface albedo (dimension less), $RL\downarrow$ is the incoming longwave radiation (W/m^2), $RL\uparrow$ is the outgoing longwave radiation (W/m^2), and ε_o is the surface thermal emissivity (dimension less).

The SEBAL algorithms were implemented in Model Maker tool of ERDAS Imagine software and intermediate derived outputs in the form of maps encompassing Leaf Area Index (LAI), Normal Difference Vegetation Index (NDVI), Soil Adjusted Vegetation Index (SAVI), Net surface radiation flux (R_n), Soil heat flux (G) and Sensible heat flux (H) were produced and analysed. The major land use classes were derived using Landsat TM 5 imagery with appropriate processing in ERDAS environment and employing supervised classification technique. In order to validate the classified images, accuracy assessment technique was carried out with ground truth data.

In SEBAL, the choice of the hot or cold pixel is the key for accurate estimation of ET and often known as an anchor pixels for deriving sensible heat flux (H) in an iterative way. During November (RS image acquisition time), since most of the crops are either harvested or due for the next growing calendar, forest area was selected as the anchor pixel for coldest temperature and the river bed as the anchor pixel for hottest temperature.

The residual evapotranspiration flux was then estimated by balancing all the sensible heat fluxes. Actual ET was computed during satellite overpass and integrated for 24-h on pixel-by-pixel basis for daily ET distribution. The reference ET (ET_r) was estimated from weather station data of ICAR-IISWC, Dehradun located at Selaqui Farm using Penman Monteith method. Reference ET acts as a base for estimating daily 24 hour ET values. Table 1 shows the weather situation in Doon valley on November 13, 2010.

Surface Radiation Balance Equation

The first step in the SEBAL procedure is to compute the net surface radiation flux (R_n) using the surface radiation balance equation:

$$R_n = (1-\alpha)\, R_{S\downarrow} + R_{L\downarrow} - R_{L\uparrow} - (1-\varepsilon_o)R_{L\downarrow} \quad \ldots(3)$$

This was accomplished in a series of steps using the ERDAS Model Maker tool to compute the terms in the above equation. A flow chart of the process is shown in Fig. 3. The computer model number used for each computation is given along with the variable name. The computation steps begin at the bottom of the figure with

Table: 1
Weather condition of November 13, 2010 in Selaqui meteorological station

Rain (mm)	Max. Temp (^{0}C)	Min. Temp (^{0}C)	RH (%)	Wind speed (m/s)	Sunshine (hr)	Pan (mm)
0	27.5	7.2	59	0.2	7.9	2.6

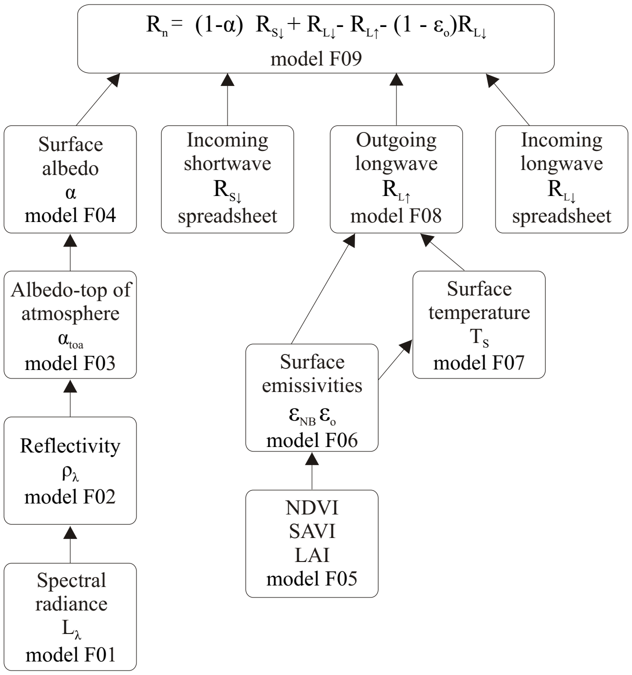

Fig. 3 Flow chart for computation of R_n

model F01 and continue upward to model F09 for the computation of R_n. The two terms $R_{S\downarrow}$ and $R_{L\downarrow}$ were computed with a spreadsheet.

24-Hour Actual Evapotranspiration (Et_{24})

After estimation of R_n, G and H; λ_{ET} (W/m^2) *i.e.* latent heat flux from the surface due to evapotranspiration was estimated as a residual value of all the sensible heat flux terms giving rise to an instantaneous value of ET for the time of satellite overpass. Therefore, instantaneous ET value in equivalent evaporation depth is computed as:

$$ET_{inst} = 3600\frac{\lambda_{ET}}{\lambda} \quad \ldots (4)$$

Where, ET_{inst} is the instantaneous ET (mm hr^{-1}) and λ is the latent heat of vaporization (J kg^{-1}) and reference ET fraction (ET_rF) is computed as:

$$ET_rF = \frac{ET_{inst}}{ET_r} \quad \ldots (5)$$

This ET_rF is similar to K_c (Crop coefficient) when multiplied with 24 h Reference ET gives actual evapotranspiration. Generally, ET_rF values ranges within 0 to 1. For completely dry pixel, ET = 0 and ET_rF = 0. A well established field of alfalfa or corn can occasionally have an ET slightly greater than ET_r and therefore $ET_rF > 1$, perhaps up to 1.1. However, ET_r generally represents an upper bound on ET for well-watered vegetation. Negative values for ET_rF can occur in SEBAL due to systematic errors caused by various assumptions made earlier in the energy balance process.

The actual evaporation is calculated in SEBAL from the instantaneous evaporative fraction, Λ, and the daily averaged net radiation, R_{n24}. The evaporative fraction Λ is estimated using following formula:

$$\Lambda = \frac{\lambda E}{R_n - G_0}$$

Finally, ET_{daily} (=ET_a) was computed using the equation:

$$ET_{daily} = \frac{86400\ \Lambda\ (R_{n24} - G_{24})}{\lambda}$$

Where, R_{n24} is daily net radiation (W/m^2), G_{24} is daily soil heat flux (W/m^2), and λ is the latent heat of vaporization (J kg^{-1}).

3. RESULTS AND DISCUSSION

Digital Elevation Model (DEM)

The ASTER DEM (30 m) was used for elevation data (Fig. 4). The elevation varies between 325 m and 2756 m with a mean value of 835 m. The higher standard deviation of 439 m suggested that the variation within the watershed is quite high.

Land Use Classification

The classified landuse image presented in Fig. 5 with an overall accuracy of 92.5% and Kappa coefficient of 0.9143 revealed that out of the 1684 sq-km of the area, major area comes under dense forest (28.5%) with a cumulative area

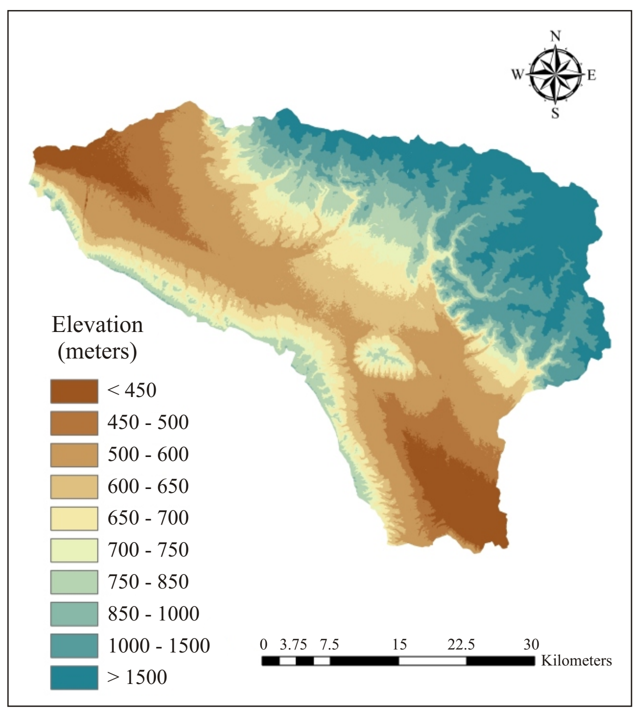

Fig. 4. ASTER DEM clipped with watershed boundary

under forest estimated to be around 37%. The urbanisation in the recent past has come up heavily with total representation had shored up to 15% of the total study area (26934 ha). Agriculture in plains covers about 3.5% area whereas terraced agriculture and agro-forestry systems has a major share (29%). The detailed classification and their areas for the study region are given in Table 2.

Reference ET Values

The reference ET serves as the base for estimating the absolute value of actual ET. Since SEBAL estimates instantaneous ET and the data was available at a daily time step, the ET was scaled as the daily temperature variation and the reference ET was estimated as 4.2 mm day^{-1}.

Vegetation Indices and Evapotranspiration (Et_a)

Spatial variation of vegetation indices was represented in Fig. 6. The areas along with the river located in middle part of the valley represent low vegetation index of ranges from 0.14 to 0.22 whereas forest areas on top of the hills showing high vegetation density ranges from 0.6 to 0.65. Fig. 7 represents the map showing the spatial variation of surface temperature in the study area with the location of hottest anchor pixel and coldest anchor pixel. The bare and barren areas and river bed with rock cover show high surface temperature of more than 30^{0}C whereas lush green areas and agriculture shows lower surface temperature of 20^{0}C.

Fig. 8 illustrates the spatial variation of ET over the study area. From Table 3 it can be seen that the average ET for the study area was about 4.29 mm day^{-1} with urban areas

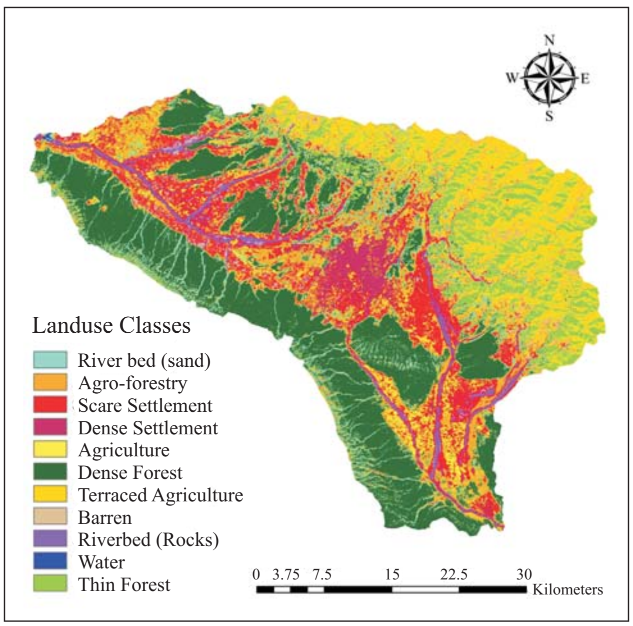

Fig. 5. Land use Classification of Doon valley

Table: 2
Aerial coverage of various landuse systems in the study area

S.No.	Class Name	Area (ha)	Area (%)
1	Riverbed (Sand)	13603	8.1
2	Agro Forestry	23495	13.9
3	Scarce Settlement	16710	9.9
4	Dense Settlement	10224	6.1
5	Agriculture (Plain land)	5852	3.5
6	Dense Forest	47991	28.5
7	Terrace Agriculture	25332	15.0
8	Barren land	5453	3.2
9	Riverbed (Rocks)	4631	2.7
10	Water	242	0.1
11	Thin Forest	14925	8.9
	Total	168458	100.0

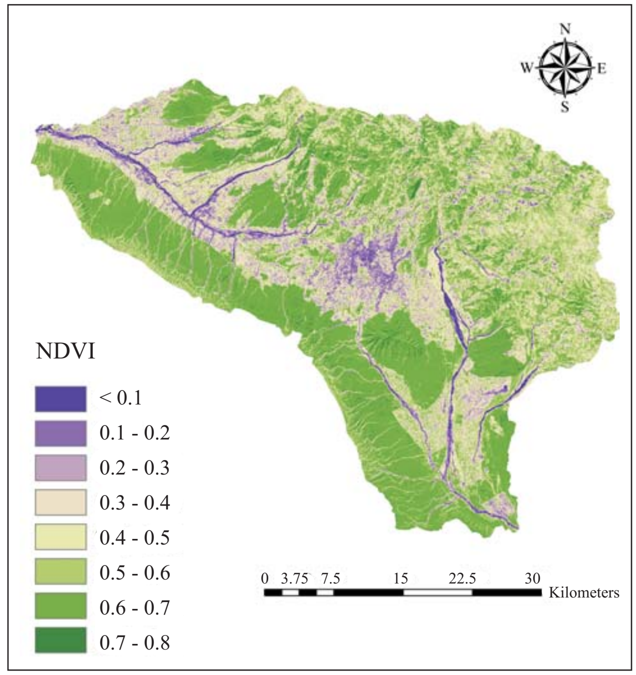

Fig. 6. NDVI map of the study area

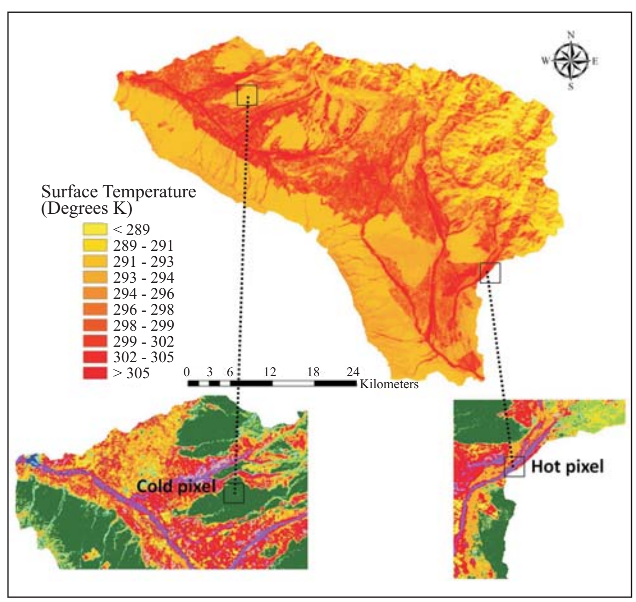

Fig. 7. Spatial variation of surface temperature in the study area with selected hot and cold pixel

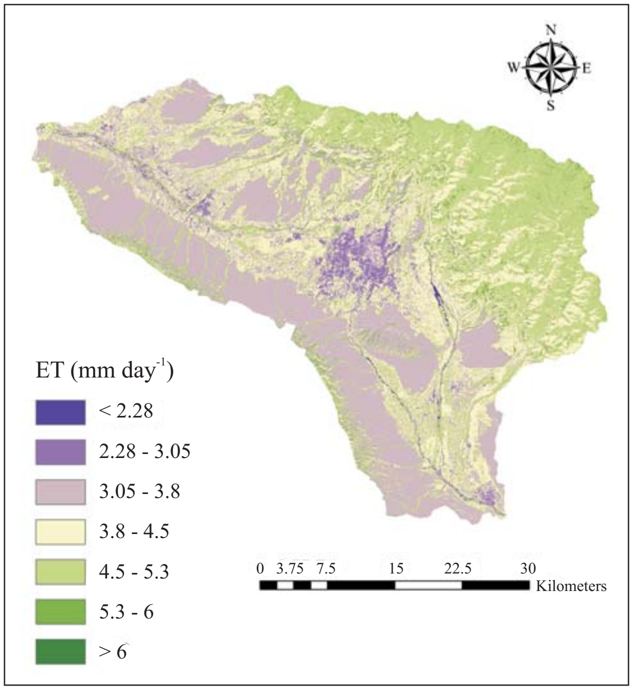

Fig. 8. Evapotranspiration map of the study area

Table: 3
Daily ET value in major land use system

Land use system	Mean ET (mm day^{-1})	Std. Dev.
River/Water body	4.6	0.24
Agro-forestry	4.1	0.17
Scare Settlement	3.9	0.13
Dense Settlement	3.3	0.22
Agriculture	4.4	0.14
Dense forest	3.7	0.13
Terraced agriculture	4.9	0.11
Barren	4.5	0.15
Thin forest	4.5	0.11

falling in less value of about 3.32 mm day^{-1}. Since the satellite image of the study area was acquired in morning, daily ET variation for different land use system is not significantly visible. The terraced agricultural area shows higher ET values (4.94 mm day^{-1}) as compared to forest areas with dense vegetation (3.72 mm day^{-1}). The River/water surface leading to free surface evaporation was estimated more than 4 mm day^{-1}.

Variation of ET in mm day^{-1} in relation to NDVI and surface temperature in ^{0}C for the different land use system were compared and presented in Fig. 9. From this figure, it can be noted that during satellite overpass time on November 13, 2010, river/water body was having high surface temperature of about 26.89^{0}C and the estimated ET from the same landuse was mainly contributed from evaporation which is about 4.6 mm day^{-1}. On the other hand, forest area shows average surface temperature of 19.77^{0}C with high vegetation index (0.7) and ET value (4.12 mm day^{-1}).

Average ET_a was computed by taking the pixel values of wheat fields of Selaqui Meteorological station. Table 4 shows the average value of daily actual ET of these fields, ETo, and Etc and ET pan of Selaqui stations. It was found that ETo (PET), ET_c and SEBAL ET_a values are almost

Table: 4
Comparison of ET pan, ET_o, ET_c and Daily ET actual, (mm day^{-1})

	Location of meteorological station	Selaqui Farm (30^0 20' N, 77^0 52' E)
13-Nov-2010	Pan Evaporation (Met. Station)	2.6
	ET_0 (Penman Monteith method)	4.2
	ET_c (K_c= 1.15)	4.83
	Landsat 5 TM (SEBAL)	4.45

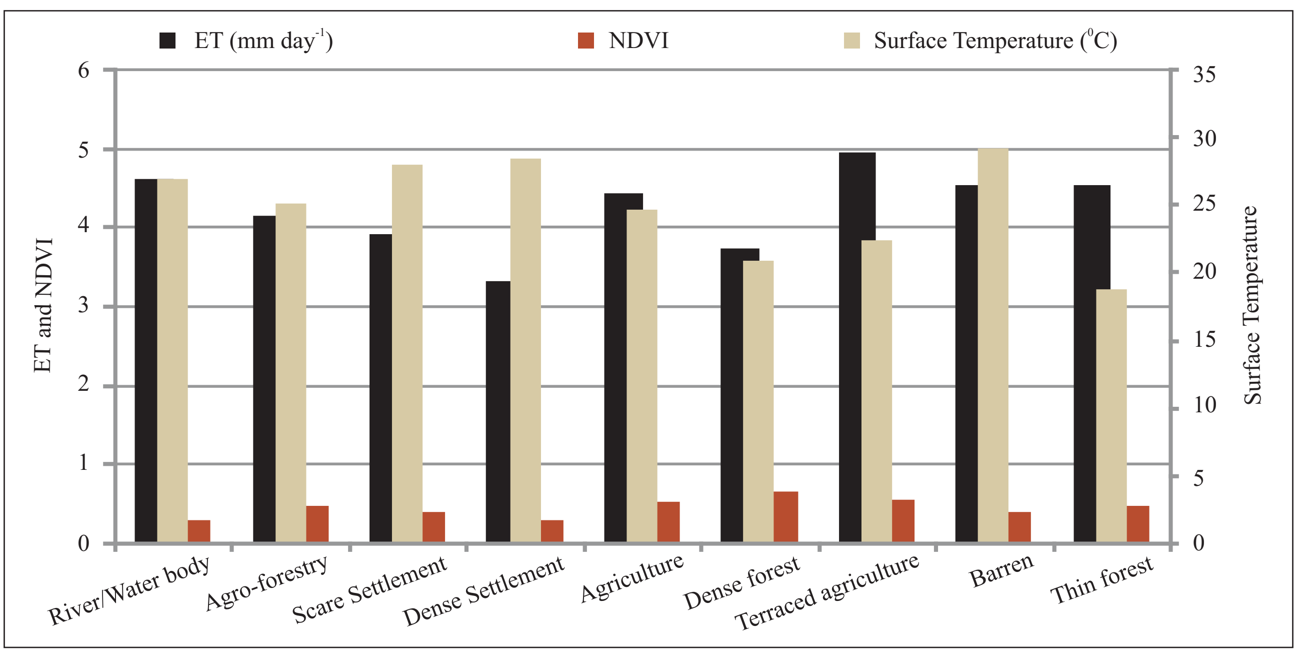

Fig. 9. Comparison between ET, NDVI and Surface temperature (Ts) during satellite overpass time

equal on the acquisition days of the landsat image. However, ET pan on that day is found quite less as compare to other values. The probable reason of this variation may be attributed to poor maintenance and lack of accurate measurement. However, the SEBAL estimated ET_a values may be validated with more ground truth points for further use.

4. CONCLUSIONS

This study was attempted to examine the SEBAL technique for mapping spatial variation of actual evapotranspiration over the Doon Valley region. The technique uses optical satellite imagery and the SEBAL algorithm to estimate ET_a on the satellite overpass day. The actual evapotranspiration (ET_a) was estimated using SEBAL mode land its spatial variation were compared over different land covers. Agriculture terrace shows the highest evapotranspiration (4.94 mm day^{-1}) as compared to other land covers. However, the method suggested that in the event of scarce ground base hydrological data, SEBAL technology can serve a quick tool to estimate ET and the ensemble of ET over a year can be utilised to plan the water resources efficiently. Though this study just showcased an application of SEBAL technique using Satellite imageries, future studies may require ground validation of this technique using the network of field lysimeters and calibrating hydrological models in ungauged watersheds using ET values as observed variables.

REFERENCES

Alexandridis, T. and Chemin, Y. 2001. Irrigation water consumption through remote sensing: Comparison at different scales in Zhanghe irrigation system, China. Presented in First International Conference on "*Water Resources Management*". Halkidiki, Greece, 10 p.

Allen, R.G., Pereira, L.S., Raes, D. and Smith, M. 1998. Crop Evapotranspiration. *Food and Agric. Organ. of the U. N. (FAO),* Rome, Italy. ISBN 92-5-104219-5. 290 p.

Bandara, K.M.P.S. 2006. Assessing irrigation performance by using remote sensing. Doctoral thesis, Wageningen University, Wageningen, The Netherlands.

Bastiaanssen, W.G.M., Noordman, E.J.M., Pelgrum, H., David, G., Thoreson, B.P. and Allen, R.G. 2005. SEBAL model with remotely sensed data to improve water resources management under actual field conditions. *J. Irrig. Drain. Eng.,* 131:85-93.

Bastiaanssen, W.G.M. 2000. SEBAL-based sensible and latent heat fluxes in the irrigated Gediz Basin, Turkey. *J. Hydrol*., 229:87-100.

Bastiaanssen, W.G.M., Ahmad, M.D. and Chemin, Y. 2002.Satellite surveillance of evaporative depletion across the Indus Basin. *Water Resour. Res.,* 38(12): 1273-1281.

Bastiaanssen, W.G.M., Menenti, M., Feddes, R.A. and Holtslag, A.A.M. 1998. A remote sensing surface energy balance algorithm for land (SEBAL) 1: Formulation. *J. Hydrol.,* 212:198-212.

Bastiaanssen, W.G.M., Noordman, E.J.M., Pelgrumm, H., Davids, G., Thoreson, B.P. and Allen, R.G. 2005. SEBAL model with remotelysensed data to improve water-resources management under actual field conditions. *J. Irrig. Drain. Eng.,* 131(1): 85-93.

Brutsert, W. 1979. Heat and mass transfer to & from surface with complete vegetation similar permeable roughness. *Bound. Layer Meteor.,* 16:365-388.

Doorenbos, J. and Pruitt, W.O. 1977. Irrigation guidelines for computing crop water requirements. Irrigation and Drainage paper No. 24, FAO, Rome, Italy.

Farah, H.O., Bastiaanssen, W.G.M. and Feddes, R.A. 2004. Evaluation of the temporal variability of the evaporative fraction in a tropical watershed. *Int. J. Appl. Earth Obs. Geoinf.,* 5:129-140.

Jana, C., Alam, N.M., Shrimali, S.S., Kumar, G., Ghosh, B.N. and Mishra, P.K. 2015. Rainfall extremity in Doon Valley of Uttarakhand reorienting Agricultural Management. *Int. J. Agril. Stat. Sci.,* 11(2): 425-431.

Kustas, W.P. and Norman, J.M. 1996.Use of remote sensing for evapotranspiration monitoring over land surfaces. *Hydrol. Sci. J.,* 41(4):495-516.

Kustas, W.P., Diak, R. and Moran, M.S. 2003. Remote sensing of evaporation. In Stewart, B.A. and Howell, T.A. (Eds.) *Encyclopedia of Water Science*s. Marcell Dekker, New York. pp. 267-274.

Liou, Y.A. and Kar, S.K. 2014. Evapotranspiration Estimation with Remote Sensing and Various Surface Energy Balance Algorithms-A Review. Energies. 7: 2821-2849; doi:10.3390/en7052821.

Majnooni-Heris, A., Sadraddini, A.A., Nazemi, A.H., Shakiba, M.R., Neyshabouri, M.R. and Hakki, T.I. 2012. Determination of single and dual crop coefficients and ratio of transpiration to evapotranspiration for canola. *Ann. Biol. Res.,* 3(4):1885-1894.

Papadavid, G., Hadjimitsis, D.G., Toulios, L. and Michaelides, S. 2013. A Modified SEBAL Modeling Approach for Estimating Crop Evapotranspiration in Semi-arid Conditions. *Water Resour. Manag*., 27:3493-3506.

Petra, J.G., Hellegers, J., Soppe, R., Perry, C.J., Bastiaanssen, W.G.M. 2010. Remote Sensing and Economic Indicators for Supporting Water Resources Management Decisions. *Water Resour. Manag.,* 24:2419-2436.

Rogers, J.S., Allen, L.H. Jr. and Calvert, D.V. 1983. Evapotranspiration from a humid-region developing citrus grove with a grass cover. *Trans. ASAE,* 26:1778-1792.

Spiliotopoulos, M., Loukas, A. and Vasiliades, L. 2008. Actual evapotranspiration estimation from satellite-based surface energy balance model in Thessaly, Greece. EGU General Assembly, 13-18 April 2008, Vienna, Austria, Geophysical Research Abstracts. 10.

Tuya, S., Batjargal, Z., Kajiwara, K., and Honda, Y. 2005. Satellite-derived estimates of evapotranspiration in the arid and semi-arid region of Mongoliá. *Int. J. Environ. Stud.,* 62(5): 517-526.

Zohu, X., Bi, S., Yang, Y., Tina, F. and Ren, D. 2014. Comparison of ET estimations by the three-temperature model, SEBAL model and eddy covariance observations. *J. Hydrol.,* 519:769-776.